Proceedings of *RAGtime 17–19, 17–19/23–26 Oct., 1–5 Nov., 2015/2016/2017, Opava, Czech Republic*
Z. Stuchlík, G. Török and V. Karas, editors, Silesian University in Opava, 2017, pp. 223–235

223

Escape cones of null-geodesics from the interior of rotating compact stars

Jaroslav Vrba,[1a+] Martin Urbanec[1b] and Zdeněk Stuchlík[1a]

[1]Institute of Physics, Faculty of Philosophy & Science, Silesian University in Opava
  Bezručovo nám. 13, CZ-746 01 Opava, Czech Republic
[a]Research Centre for Theoretical Physics and Astrophysics
[b]Research Centre for Computational Physics and Data Processing
[+]jaroslav.vrba@fpf.slu.cz

ABSTRACT

In this work we present investigation of the escape cones of null-geodesics from the interior of rotating homogeneous compact stars in the model, where only terms linear in the star's rotational frequency are assumed. We focus on the single model of the star with particular radius $R = 2.8M$ (using units in which $c = G = 1$) rotating with different values of angular momentum J. We vary the position of the isotropically radiating source both in radial and latitudinal direction and we show the impact of the position and the rotational rate on the shape of the escape cone of null-geodesics. We find that even for small rotational rate corresponding to $j = J/M^2 = 0.1$ the impact on the escape cones is rather strong. The escape cones are no longer symmetrical around radial direction, and it is clearly seen that the radiation in the direction of the rotation can easily reach the infinity. On the other hand, the radiation in the direction opposite to the rotation will be trapped in the interior of the star. We discuss possible astrophysical relevance of our results.

Keywords: Compact object – axially symmetric spacetime – trapped null-geodesic – effective potential – escape cone

1 INTRODUCTION

Compact stars are general-relativistic objects with internal structure where general relativity plays key role in governing both their structure and astrophysical phenomena in their surroundings. Their central densities reach values that are not achievable in any terrestrial experiment and they serve as unique laboratories for nuclear physics and gravitational physics. Usually by compact stars we mean either neutron stars or strange stars. Neutron stars are made of neutrons, protons and electrons that are in β−equilibrium (see e.g. S.L. Shapiro and S.A. Teukolsky, (1983)), while strange stars are consisting of up, down and strange quarks that are deconfined (Witten, 1984). Different descriptions of microphysics of the interior matter transform into different global properties of the star for the same values of central density. Main gross properties of the compact star are its gravitational mass M, radius R and if the star is rotating with given angular velocity Ω, also its

angular momentum J and quadrupole moment Q (see e.g. Urbanec et al. (2013) for impact of equation of state on the gross properties of the compact star).

Null-geodesics and their trapping have been investigated in various contexts in many previous works (Abramowicz et al., 1997; Stuchlík et al., 2009, 2011, 2012; Novotný et al., 2017; Völkel and Kokkotas, 2017). In the non-rotating case, the null-geodesics can be trapped in the interior of the star if the star's radius R is bellow the position of circular photon orbit, i.e. if $R < 3M$[1]. However, most of the models of neutron stars calculated using realistic equations of state are having radius $R > 3M$ (see e.g. Figure 1 in Urbanec et al. (2013)). Rotation of the compact star is going to affect external space-time and therefore the position of the photon orbit.

Within this work we are going to focus on the very simple model, where the star is homogeneous with constant energy-density ρ and the rotation is taken as a perturbation of spherically symmetric Schwarzschild metric. We are going to keep the terms that are linear in the star's angular velocity Ω only. This is the same approach as the linearization of the Hartle-Thorne model (Hartle and Thorne, 1968). We first study the effective potential inside and close-to compact object for star with $R = 2.8M$ to demonstrate the impact of rotation. Later we use the concept of the escape cones introduced in Schee et al. (2005); Stuchlík and Schee (2010) to demonstrate directions of the null-geodesics that are trapped by the gravity of a compact object.

Relevance of this research has increased after the first detection of gravitational-wave signal from merging neutron stars (Abbott et al., 2017b) that has been observed with its optical counterparts (Abbott et al., 2017a,c). Both gravitational-waves and electromagnetic-waves are moving along null geodesics and if the neutron star is formed after the coalescence, it may be very heavy and may rotate very rapidly. Combination of high mass and high rotational rate will lead to the existence of counter-rotating circular photon orbit in the exterior space-time of the compact star causing part of the geodesics (and therefore gravitational waves) to be trapped in the interior of the compact star.

The paper is organized as follows. In Section 2, we focus on the spherically symmetric case. We present effective potential and the trapping of null-geodesics in the similar way as in Stuchlík et al. (2009), and we introduce escape cones in Section 2 as well. In Section 3 we investigate the influence of rotation on possible trapping of null-geodesics using both the profiles of effective potential and the escape cones. Section 4 contains our conclusions.

2 SPHERICALLY SYMMETRIC SPACETIME

In this section we recap main concepts of Stuchlík et al. (2009) and we introduce the escape cones of null-geodesics in this context. This work deals with model of the homogeneous compact star.

We are interested in the toy model to be able to perform most of the calculations analytically and to use it in the future as a testbed for more advanced calculations.

---

[1] We are using units in which $c = G = 1$ thorough this paper.

Line element of spherically symmetric space-time can be written in spherical coordinates as (Schwarzschild, 1999)

$$ds^2 = -e^{2\Phi(r)}dt^2 + e^{2\Psi(r)}dr^2 + r^2(d\theta^2 + \sin^2\theta d\phi^2). \tag{1}$$

Assuming constant energy-density ρ, we can write the metric coefficients in the form

$$(-g_{tt})^{1/2} = e^\Phi = \frac{3}{2}Y_1 - \frac{1}{2}Y(r), \qquad (g_{rr})^{1/2} = e^\Psi = \frac{1}{Y(r)}, \tag{2}$$

where

$$Y(r) = \sqrt{1 - \frac{r^2}{a^2}}, \qquad Y_1 = Y(R) = \sqrt{1 - \frac{R^2}{a^2}}, \tag{3}$$

$$\frac{1}{a^2} = \frac{3}{8}\pi\rho = \frac{2M}{R^3}, \tag{4}$$

and M and R are the mass and the radius of the compact star.

It is convenient to use the tetrad formalism. We can rewrite Equations (1)-(4) as

$$ds^2 = [\omega^{(t)}]^2 + [\omega^{(r)}]^2 + [\omega^{(\theta)}]^2 + [\omega^{(\phi)}]^2, \tag{5}$$

where

$$\omega^{(t)} = e^\Phi dt, \quad \omega^{(r)} = e^\Psi dr, \quad \omega^{(\theta)} = r d\theta, \quad \omega^{(\phi)} = r\sin\theta d\phi. \tag{6}$$

Relations between vectors and co-vectors are written as

$$\omega_\mu^{(\alpha)} e_{(\beta)}^\mu = \delta_{(\beta)}^{(\alpha)} \quad \text{and} \quad e_{(\alpha)}^\mu \omega_\nu^{(\alpha)} = \delta_\nu^\mu. \tag{7}$$

We use this formalism to project 4-momentum of the mass-less particle k^μ to the local frame as $k^{(\alpha)} = k^\mu \omega_\mu^{(\alpha)}$, $k_{(\alpha)} = k_\mu e_{(\alpha)}^\mu$.

2.1 Effective potential

The motion along null-geodesics is described by the equation of motion

$$\frac{Dk^\mu}{d\tau} = 0 \qquad \text{and} \qquad k_\mu k^\mu = 0, \tag{8}$$

where τ is the proper time. We can find two Killing fields ($\frac{\partial}{\partial t}$ and $\frac{\partial}{\partial\phi}$) and relate them to the constants of motion E and L as

$$k_t = -E \qquad \text{and} \qquad k_\phi = L. \tag{9}$$

In the spherically symmetric case, the motion takes place in a single plane that can be identified with the equatorial one and we can therefore set $\theta = \pi/2$ and $k^\theta = 0$. Combining (8) and (9) we then get

$$(k^r)^2 = \frac{1}{g_{tt}g_{rr}}E^2\left(1 - g_{tt}\frac{\lambda^2}{r^2}\right), \tag{10}$$

⏮ ◄ ► ⏭

where we introduced the impact parameter $\lambda = L/E$. The term in the brackets in the formula above needs to non-negative and this condition can be written as

$$\lambda^2 \leq V_{\text{eff}} = -\frac{r^2}{g_{tt}}, \tag{11}$$

where we have defined the effective potential V_{eff}.

The effective potential for the star with $R/M = 2.8$ is plotted in Figure 1. On the right panel of Figure 1 we see that there can be distinguished two kinds of trapping that are visualized by darker and lighter areas. If the null geodesic is described by the impact parameter $\lambda > \lambda_{\text{crit}} = \sqrt{V_{\text{eff}}(r = 3M)}$ the geodesic will be trapped under the circular photon orbit $r_{\text{ph}} = 3M$, the particle moving along it will leave the star, hit the potential barrier and will be reflected back and will enter the star later (lighter area of right panel of Figure 1). If the $\lambda > \sqrt{V_{\text{eff}}(r = R)}$ the geodesic will stay in the interior of the star permanently (darker area of right panel of Figure 1). We also see that if the particle is radiated from the radius $r < r_{\text{b}}$ there is no potential barrier for it and it will escape to the infinity. Therefore we see that the trapping of geodesics take place only in limited area of the star and that only limited part of the mass-less particles radiated from this are will be trapped. For the purpose of this work we will distinguish only between geodesics that are trapped and geodesics that can reach the infinity. A more detailed discussion of trapped areas can be found in Stuchlík et al. (2009).
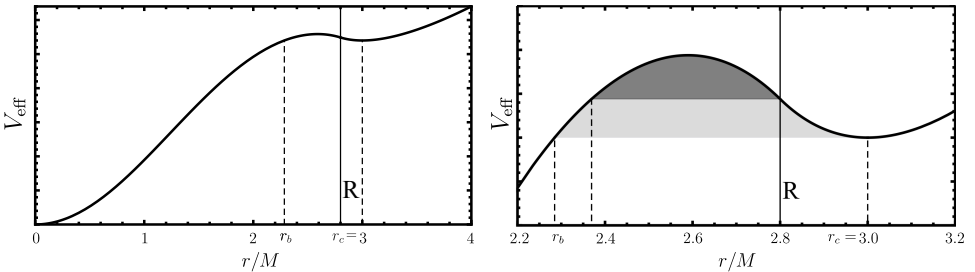
Figure 1. Effective potential of star with $R/M = 2.8$. Schematic depiction of the trapped area (right). See text for details.

2.2 Escape cones

Escape cones has been presented e.g. in Schee et al. (2005); Stuchlík and Schee (2010) and we are going to use similar approach here. Four-momentum of mass-less particles radiated from given position in the compact star can be written using directional angles (see Figure 2)

$$k^{(t)} = -k_{(t)} = 1, \tag{12}$$

$$k^{(r)} = k_{(r)} = \cos\alpha, \tag{13}$$

$$k^{(\theta)} = k_{(\theta)} = \sin\alpha\cos\beta, \tag{14}$$

$$k^{(\phi)} = k_{(\phi)} = \sin\alpha \sin\beta = \cos\gamma. \tag{15}$$

We can see that two angles are sufficient to determine the direction of the null-geodesic at the radiation point.
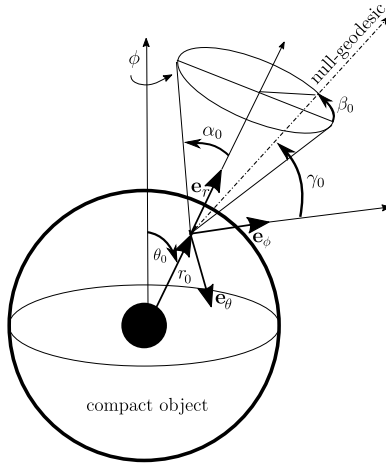
Figure 2. The definition of directional angles of null-geodesic radiated from the point with coordinates r_0, θ_0.

Now let us say we have a point emitter which emits mass-less particles that are moving along null-geodesics. The escape cone determines directions of null-geodesics which can travel to infinity. Complementary directions correspond to null-geodesics that are trapped by the gravitational field. These directions are described by angles $[\alpha,\beta]$, defined in Figure 2 and they may be plotted to a polar graph of escape cone where α is the 'radial' coordinate ($\alpha \in \langle 0,\pi \rangle$) and β is the 'polar' coordinate ($\beta \in \langle 0,2\pi \rangle$). The position of the emitter is determined by $[r_0,\theta_0]$. For instance, if we sit at any r in the equatorial plane, i.e., $[r_0,\pi/2]$ the direction (a) $[\alpha,\beta]=[0,\text{whatever}]$, points radially to infinity, (b) $[\alpha,\beta]=[\pi,\text{whatever}]$, points directly to the center and (c) $[\alpha,\beta]=[\pi/2,\pi/2]$, points perpendicularly to the radial direction in the equatorial plane in direction of the rotation (if the star would be rotating).

The typical escape cone for non-rotating objects is shown in Figure 3. This particular one has been constructed in the equatorial plane and at the radial coordinate r corresponding to the position of the maxima of the effective potential. We see that dark are that is corresponding to the trapped geodesics is symmetrical around $\alpha = \pi/2$ that is corresponding to the radiation in the direction perpendicular to the radial direction and we also see, that there is no dependency on the angle β being given by the spherically symmetric space-time.
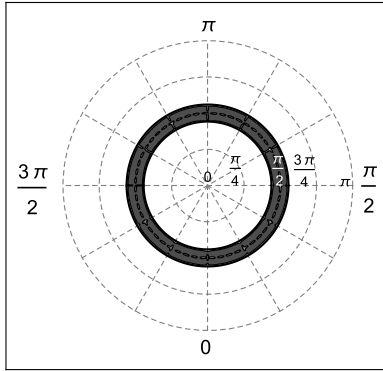
Figure 3. The escape cone produced at the maximum of the effective potential for $R/M = 2.8$. A shaded area depicts directional angles α, β for which the null-geodesics is trapped trapped .

3   AXIALLY SYMMETRIC SPACE-TIME

The main goal of this section is to examine escape cones produced in various points in the interior of the slowly and rigidly rotating compact star. We model rotating compact stars taking into account corrections up to the first order in the angular velocity of the star Ω. For description of the rotating body we will use dimension-less specific angular momentum $j = J/M^2$, where J is angular momentum of the body.

The rotating star within this approximation is described by the Lense-Thirring metric (Lense and Thirring, 1918)

$$g_{t\phi} = g_{\phi t} = -\omega(r)r^2 \sin^2(\theta), \tag{16}$$

where the diagonal components of the metric tensor $g_{\mu\mu}$ are the same as in the non-rotating case (1-4), and in addition there are cross terms that can be written as

$$ds^2 = -e^{2\Phi(r)}dt^2 + e^{2\Psi(r)}dr^2 + r^2(d\theta^2 + \sin^2\theta d\phi^2) + 2g_{t\phi}dt d\phi, \tag{17}$$

where the function $\omega(r)$ represents angular velocity of the locally non-rotating frame (LNRF). It can be calculated from relations for the angular velocity of the matter with respect to the angular velocity of LNRF $\bar{\omega}(r) = \Omega - \omega(r)$. Equation for $\tilde{\omega}(r)$ is the same as in the Hartle-Thorne model (Hartle and Thorne, 1968)

$$\frac{1}{4}\frac{d}{dr}\left(r^4 j(r)\frac{d\bar{\omega}}{dr}\right) + \frac{4}{r}\frac{d j(r)}{dr}\bar{\omega} = 0, \tag{18}$$

where

$$j(r) = \sqrt{\frac{-1}{g_{tt}g_{rr}}}. \tag{19}$$

For deeper analysis of the problem and inclusion of higher order terms see Hartle (1967) and Hartle and Thorne (1968).

3.1   Tetrad formalism

The tetrad formalism is very useful for the case of rotating object. The LNRF frame is in this formalism given by relations

$$\omega^{(t)} = \left\{ \sqrt{-\omega(r)g_{\phi t} - g_{tt}}, 0, 0, 0 \right\}, \tag{20}$$

$$\omega^{(r)} = \left\{ 0, \sqrt{g_{rr}}, 0, 0 \right\}, \tag{21}$$

$$\omega^{(\theta)} = \left\{ 0, 0, \sqrt{g_{\theta\theta}}, 0 \right\}, \tag{22}$$

$$\omega^{(\varphi)} = \left\{ -\omega(r) \sqrt{g_{\phi\phi}} \sin\theta, 0, 0, \sqrt{g_{\phi\phi}} \right\}. \tag{23}$$

We transform it using the Lorentz transformation Λ to the frame rotating with the object (with angular velocity Ω).

$$\Lambda(\bar{\omega}) = \begin{pmatrix} \gamma & 0 & 0 & -\gamma\bar{\omega} \\ 0 & 1 & 0 & 0 \\ 0 & 0 & 1 & 0 \\ -\gamma\bar{\omega} & 0 & 0 & \gamma \end{pmatrix}, \tag{24}$$

where $\gamma = 1/\sqrt{1 - \bar{\omega}^2}$ is Lorentz factor. We can finally write $\bar{\omega}$ as[2]

$$\bar{\omega} = \frac{U^{(\phi)}}{U^{(t)}} = \frac{\omega_\mu^{(\phi)} U^\mu}{\omega_\mu^{(t)} U^\mu}. \tag{25}$$

3.2   Effective potential

The effective potential related to null-geodesics in the space-time described by line-element (17) can be derived using the Lagrangian (see e.g. Chandrasekhar (1983))

$$2\mathcal{L} = g_{tt}\dot{t}^2 + g_{rr}\dot{r}^2 + g_{\theta\theta}\dot{\theta}^2 + g_{\phi\phi}\dot{\phi}^2 + 2g_{t\phi}\dot{\phi}\dot{t}. \tag{26}$$

The radial part of the effective potential reads

$$V_{\text{Reff}} = 2g^{t\phi}g_{\theta\theta}\lambda - g^{tt}g_{\theta\theta}, \tag{27}$$

and the latitudinal part takes the form

$$V_{\text{Teff}} = \frac{\lambda^2}{\sin^2\theta}, \tag{28}$$

where we use the impact parameter

$$\lambda = \frac{L}{E} = \frac{k_\phi}{-k_t} = \frac{\omega_\phi^{(\mu)} k_{(\mu)}}{-\omega_t^{(\mu)} k_{(\mu)}}. \tag{29}$$

---

[2]   Index in bracket is expressed in local frame.
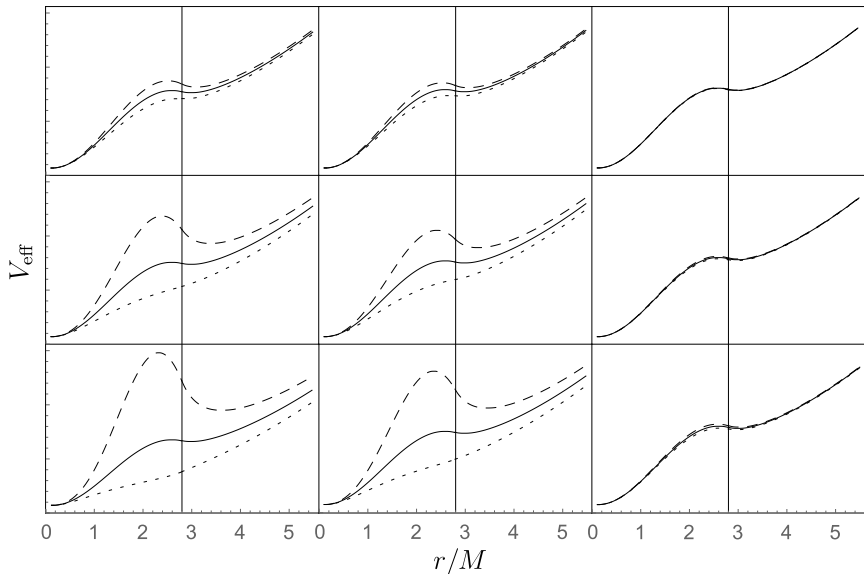
Figure 4. Effective potentials of the radial part of null-geodesic for configuration with $R/M = 2.8$. First column corresponds to $\theta = \pi/2$, second to $\pi/4$, and third to $\pi/1000$. In first row specific angular momentum of the star is $j = 0.1$ in the second row $j = 0.4$ and in the third row $j = 0.7$. Dashed lines are corresponding to counter-rotating geodesics while the dotted lines to co-rotating ones. Full lines are plotted for comparison and they correspond to the non-rotating case, where $j = 0$.

We can notice that if the rotation vanishes (i.e $g_{t\phi} = 0$), effective potentials given by Eqs. (11) and (27) are identical. The resulting effective potentials are illustrated in Figure 4, where we plot the effective potential separately for co-rotating particles (dotted line) and for counter-rotating particles (dashed line). For comparison, we plot effective potential for non-rotating configuration as well (solid line).

3.3 Escape cones

Detailed description of a construction of the light escape cones for Kerr black holes and naked singularities can be found in Schee et al. (2005); Stuchlík and Schee (2010). Here, we adopt the main idea of it in the context of slowly-rotating compact stars. Constants of motion (9) fully determine the direction angles as they were defined in Figure 2. The relation (29) connects constant λ and angle γ. For trapped geodesics the constant λ is limited by the condition $V_{\text{Reff}} > V_{\text{Teff}}$, coming from the separation of equations of motion. Using relation

$$\cos\alpha = \frac{k^{(r)}}{k^{(t)}} = \frac{\omega_\mu^{(r)} k^\mu}{\omega_\mu^{(t)} k^\mu}, \tag{30}$$

⏮ ◀ ▶ ⏭
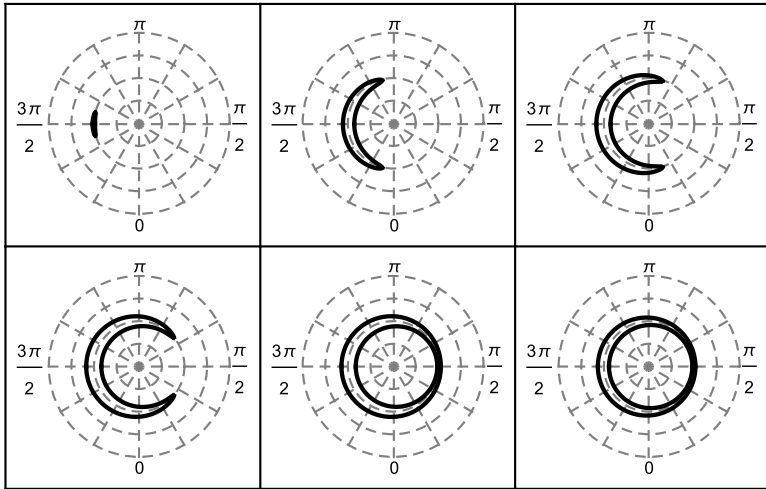
Figure 5. Escape cones of configuration with $R/M = 2.8$ and specific angular momentum $j = 0.1$. Cones are produced at $\theta_0 = \pi/2$ and at points where $r_0 = \{2.285, 2.388, 2.491, 2.594, 2.697, 2.8\}M$.

that relates directional angles α and γ. In order to null-geodesic being trapped, the value of λ^2 has to be in the shaded region in Figure 1 (see also Eq. (27)), i.e. λ^2 has to be bigger than the minimum of the effective potential in the exterior space-time. The condition when λ^2 is equal to the value of minimum of effective potential determines a critical value of angle α separating the trapped null-geodesics and null-geodesics that can reach infinity. An angle β is determined from Eq. (15).

This procedure is repeated for all allowed values of λ and values $[\alpha, \beta]$ are plotted in a graph as the escape cone.

We now create a set of escape cones in different positions r_0 of the rotating body. We vary rotating rate and initial r_0 in the equatorial plane ($\theta = \pi/2$) for the compact star with $R/M = 2.8$ rotating with $j = 0.1$, 0.4 and $j = 0.7$ and we plot the resulting escape cones in Figures 5–7. We can see that even for very low rotational rate, the impact on the escape cones is rather strong. We see that the trapped areas are more dominant in the left half of the escape cones, corresponding to the geodesics radiated in the opposite direction with respect to the rotation. We also see that with increasing rotational rate the smallest selected values of r_0 (corresponding to the top left escape-cone) is decreasing ($r_0 = 2.285M$ for $j = 0.1$, while $r_0 = 1.68M$ for $j = 0.7$). This is corresponding to the situation that is clearly seen of Figure 4 bottom, left, where we see that counter-rotating geodesics are trapped for much smaller values r_0 and that co-rotating geodesics can not be trapped for such a high values of rotational rate.

We will now investigate impact of latitudinal coordinate θ_0 on the escape cones of null-geodesics. We present the results on Figures 8, 9. We can see that as we are decreasing θ, i.e. as we are approaching the rotational axis, the escape cones of null-geodesics are
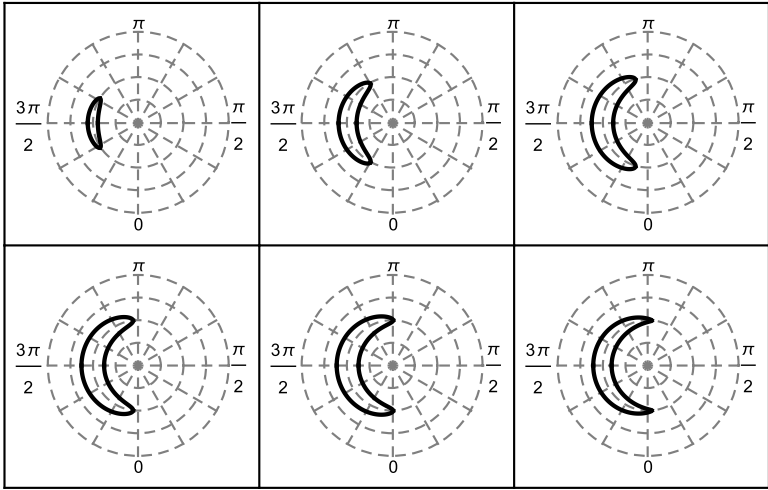
Figure 6. Escape cones of configuration with $R/M = 2.8$ and specific angular momentum $j = 0.4$. Cones are produced at $\theta_0 = \pi/2$ and at points where $r_0 = \{1.785, 1.988, 2.191, 2.394, 2.597, 2.8\}M$.
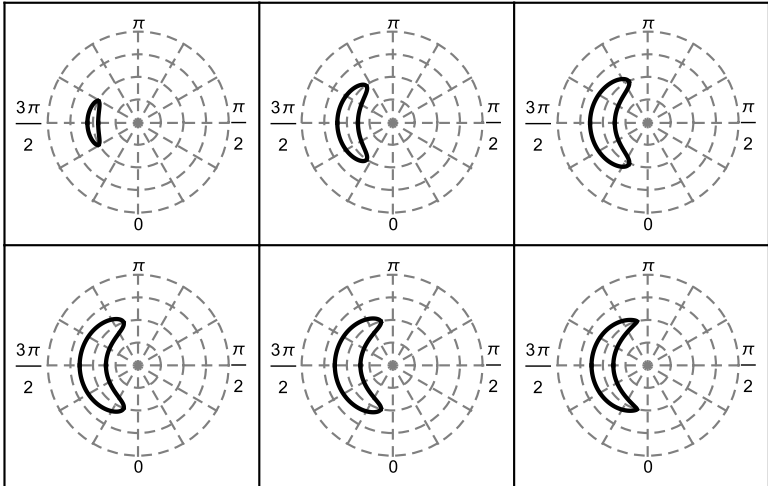
Figure 7. Escape cones of configuration with $R/M = 2.8$ and specific angular momentum $j = 0.7$. Cones are produced at $\theta_0 = \pi/2$ and at points where $r_0 = \{1.68, 1.904, 2.128, 2.352, 2.576, 2.8\}M$.

becoming more symmetrical as expected. This is of course natural result since the impact of rotation is becoming negligible as one is approaching the rotational axis.
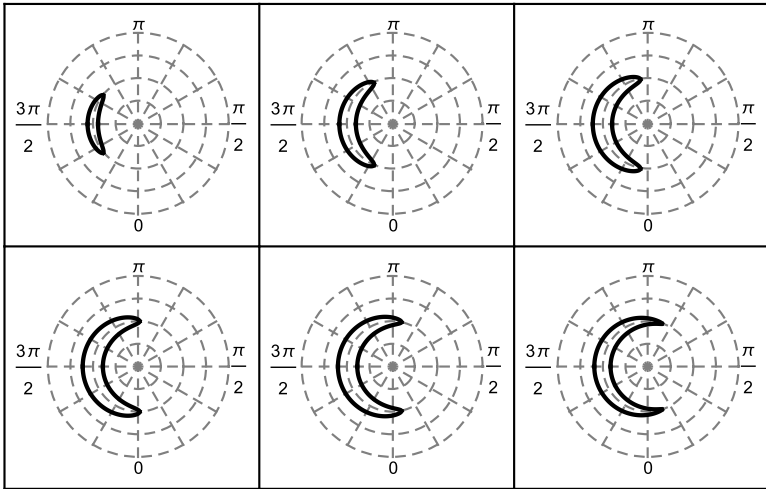
Figure 8. Escape cones of configuration with $R/M = 2.8$ and specific angular momentum $j = 0.4$. Cones are produced at $\theta_0 = \pi/4$ and at points where $r_0 = \{1.889, 2.071, 2.253, 2.435, 2.617, 2.8\}M$.
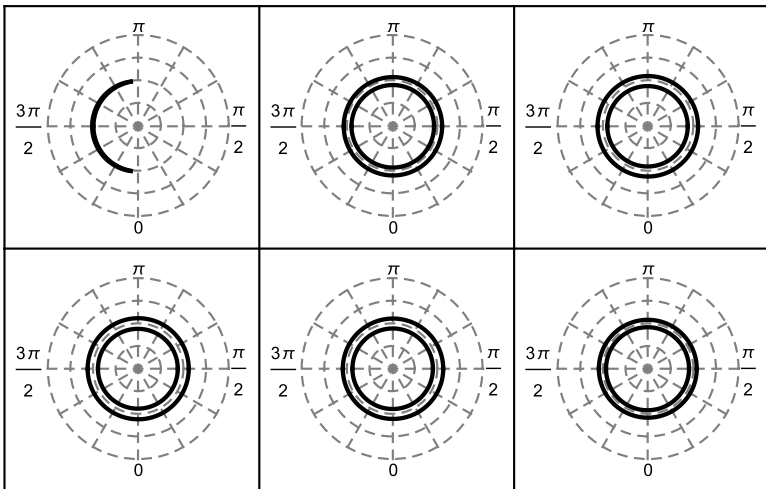
Figure 9. Escape cones of configuration with $R/M = 2.8$ and specific angular momentum $j = 0.4$. Cones are produced at $\theta_0 = \pi/1000$ and at points where $r_0 = \{2.285, 2.388, 2.491, 2.594, 2.697, 2.8\}M$.

4 CONCLUSIONS

We studied escape cones of null-geodesics from the interior of the rotating homogeneous compact stars in the limit of slow rotation. We have shown that the rotation has significant

impact on the existence and on the shape of the escape cones. Rotation separates the null-geodesics into two families - the ones that are directing in the same direction as the rotation (co-rotating ones) and the ones that are directing in the opposite direction (counter-rotating ones). The mass-less particles that will move in the co-rotating direction can easily escape the gravitational field than the particles moving in the counter-rotating direction. This may lead to additional slow-down of the rotating compact-star.

We also investigated the impact of the position of the radiating source on the escape cones of null-geodesics. We plotted escape cones of null-geodesics for positions at various radial and latitudinal coordinate. We have seen, that as one is approaching the rotational axis, the impact of rotation is becoming less important.

Our main motivation was to see the impact of rotation on the trapping of null-geodesics inside the rotating compact star. Rotation allow the trapping for stars having radius $R > 3M$ because the position of the counter-rotating circular photon orbit is shifted and can therefore be relevant for models of compact stars with realistic equations of state. More studies in this field are planned in the future and model presented in this paper will be used as testbed for more sophisticated calculations.

ACKNOWLEDGEMENTS

REFERENCES

Abbott, B. P., Abbott, R., Abbott, T. D., Acernese, F., Ackley, K., Adams, C., Adams, T., Addesso, P., Adhikari, R. X., Adya, V. B. and et al. (2017a), Gravitational Waves and Gamma-Rays from a Binary Neutron Star Merger: GW170817 and GRB 170817A, *Astrophys. J. Lett.*, **848**, L13, arXiv: 1710.05834.

Abbott, B. P., Abbott, R., Abbott, T. D., Acernese, F., Ackley, K., Adams, C., Adams, T., Addesso, P., Adhikari, R. X., Adya, V. B. and et al. (2017b), GW170817: Observation of Gravitational Waves from a Binary Neutron Star Inspiral, *Physical Review Letters*, **119**(16), 161101, arXiv: 1710.05832.

Abbott, B. P., Abbott, R., Abbott, T. D., Acernese, F., Ackley, K., Adams, C., Adams, T., Addesso, P., Adhikari, R. X., Adya, V. B. and et al. (2017c), Multi-messenger Observations of a Binary Neutron Star Merger, *Astrophys. J. Lett.*, **848**, L12, arXiv: 1710.05833.

Abramowicz, M. A., Andersson, N., Bruni, M., Ghosh, P. and Sonego, S. (1997), LETTER TO THE EDITOR: Gravitational waves from ultracompact stars: the optical geometry view of trapped modes, *Classical and Quantum Gravity*, **14**, pp. L189–L194.

Chandrasekhar, S. (1983), *The mathematical theory of black holes*, Oxford/New York, Clarendon Press/Oxford University Press.

Hartle, J. B. (1967), Slowly Rotating Relativistic Stars. I. Equations of Structure, *The Astrophysical Journal*, **150**, pp. 1005–+.

Hartle, J. B. and Thorne, K. S. (1968), Slowly Rotating Relativistic Stars. II. Models for Neutron Stars and Supermassive Stars, *The Astrophysical Journal*, **153**, pp. 807–+.

Lense, J. and Thirring, H. (1918), Über den Einfluß der Eigenrotation der Zentralkörper auf die Bewegung der Planeten und Monde nach der Einsteinschen Gravitationstheorie, *Physikalische Zeitschrift*, **19**.

Novotný, J., Hladík, J. and Stuchlík, Z. (2017), Polytropic spheres containing regions of trapped null geodesics, *Phys. Rev. D*, **95**(4), 043009, arXiv: `1703.04604`.

Schee, J., Stuchlík, Z. and Jurán, J. (2005), Light escape cones and raytracing in Kerr geometry, in S. Hledík and Z. Stuchlík, editors, *RAGtime 6/7: Workshops on black holes and neutron stars*, pp. 143–155.

Schwarzschild, K. (1999), On the gravitational field of a sphere of incompressible fluid according to Einstein's theory, *ArXiv Physics e-prints*, arXiv: `physics/9912033`.

S.L. Shapiro and S.A. Teukolsky, (1983), *Black holes, white dwarfs and neutron stars*, John Wilery and Sons, New York.

Stuchlík, Z., Hladík, J. and Urbanec, M. (2011), Neutrino trapping in braneworld extremely compact stars, *General Relativity and Gravitation*, **43**, pp. 3163–3190, arXiv: `1108.5767`.

Stuchlík, Z., Hladík, J., Urbanec, M. and Török, G. (2012), Neutrino trapping in extremely compact objects described by the internal Schwarzschild-(anti-)de Sitter spacetimes, *General Relativity and Gravitation*, **44**, pp. 1393–1417.

Stuchlík, Z. and Schee, J. (2010), Appearance of Keplerian discs orbiting Kerr superspinars, *Classical and Quantum Gravity*, **27**(21), 215017, arXiv: `1101.3569`.

Stuchlík, Z., Török, G., Hledík, S. and Urbanec, M. (2009), Neutrino trapping in extremely compact objects: I. Efficiency of trapping in the internal Schwarzschild spacetimes, *Classical and Quantum Gravity*, **26**(3), pp. 035003–+.

Urbanec, M., Miller, J. C. and Stuchlík, Z. (2013), Quadrupole moments of rotating neutron stars and strange stars, *MNRAS*, **433**, pp. 1903–1909, arXiv: `1301.5925`.

Völkel, S. H. and Kokkotas, K. D. (2017), Ultra compact stars: reconstructing the perturbation potential, *Classical and Quantum Gravity*, **34**(17), 175015, arXiv: `1704.07517`.

Witten, E. (1984), Cosmic separation of phases, *Phys. Rev. D*, **30**, pp. 272–285.